S0019-1035(03)00384-1/FLA AID:7261 Vol.●●●(●●●)
ELSGMLTM(YICAR):m5 2003/12/18 Prn:8/01/2004; 16:03

yicar7261

P.1(1-8)
by:Neringa p. 1

Available online at www.sciencedirect.com

SCIENCE DIRECT®

ELSEVIER

Icarus ●●● (●●●●) ●●●–●●●

ICARUS

www.elsevier.com/locate/icarus

# TRACE observations of the 15 November 1999 transit of Mercury and the Black Drop effect: considerations for the 2004 transit of Venus

Glenn Schneider,[a,*] Jay M. Pasachoff,[b] and Leon Golub [c]

[a] *Steward Observatory, University of Arizona, 933 North Cherry Avenue, Tucson, AZ 85721, USA*
[b] *Williams College-Hopkins Observatory, Williamstown, MA 01267, USA*
[c] *Smithsonian Astrophysical Observatory, Mail Stop 58, 60 Garden Street, Cambridge, MA 02138, USA*

Received 15 May 2003; revised 14 October 2003

**Abstract**

Historically, the visual manifestation of the "Black Drop effect," the appearance of a band linking the solar limb to the disk of a transiting planet near the point of internal tangency, had limited the accuracy of the determination of the Astronomical Unit and the scale of the Solar System in the 18th and 19th centuries. This problem was misunderstood in the case of Venus during its rare transits due the presence of its atmosphere. We report on observations of the 15 November 1999 transit of Mercury obtained, without the degrading effects of the Earth's atmosphere, with the Transition Region and Coronal Explorer spacecraft. In spite of the telescope's location beyond the Earth's atmosphere, and the absence of a significant mercurian atmosphere, a faint Black Drop effect was detected. After calibration and removal of, or compensation for, both internal and external systematic effects, the only radially directed brightness anisotropies found resulted from the convolution of the instrumental point-spread function with the solar limb-darkened, back-lit, illumination function. We discuss these effects in light of earlier ground-based observations of transits of Mercury and of Venus (also including the effects of atmospheric "seeing") to explain the historical basis for the Black Drop effect. The methodologies we outline here for improving upon transit imagery are applicable to ground-based (adaptive optics augmented) and space-based observations of the 8 June 2004 and 5–6 June 2012 transits of Venus, providing a path to achieving high-precision measurements at and near the instants of internal limb tangencies.


*Keywords:* Mercury; Venus; Instrumentation

## 1. Introduction

Transits of the inner planets have historically provided the calibrations needed to convert Kepler's relative scale of distances in the Solar System to absolute ones (e.g., Van Helden, 1989–1995; Ferguson, 1999; Hughes, 2001; Pasachoff, 2000, 2002). Most important have been transits of Venus, which occur in pairs separated by 8 years, with an interval of 105.5 or 121.5 years between the pairs. Only six transits of Venus have occurred since the invention of the telescope. The first of these transits, which was predicted by Kepler, occurred on 7 December 1631, but was unobserved. This was followed by the second transit of this pair on December 4, 1639 (November 24 O.S.), predicted by Jeremiah Horrocks and observed only by him and by a friend. Transits of Mercury are more common than of Venus, and numerous reports exist in the historical literature. For example, Bevis (1742–1743), the author of an unpublished star atlas (Kilburn et al., 2003), reported on the 31 October 1736 and 25 October 1743 transits of Mercury. Bevis (1737–1738) also observed the historically unique 28 May 1737 (O.S.) occultation of Mercury by Venus, the only such event since 20 August 796 with both planets only 5° from the Sun (de Meis, 1993), and the next not occurring until 3 December 2133 (Albers, 1979).

Following later work by Halley and others, the cytherean transits of 6 June 1761 and 3 June 1769 (Figs. 1 and 2) were observed by hundreds of expeditions. Most notable, perhaps, was James Cook's expedition with Charles Green to observe the 1769 transit from Othaheite, Tahiti (Cook and Green, 1771). Their expedition led to spinoffs such as the "discovery" of New Zealand and the exploration of the east coast of Australia and Tahiti (Chapman, 1998). Tragically, however, Green along with half the crew of the Endeavour

* Corresponding author.
*E-mail address:* gschneider@as.arizona.edu (G. Schneider).

0019-1035/$ – see front matter © 2004 Published by Elsevier Inc.
doi:10.1016/j.icarus.2003.11.020

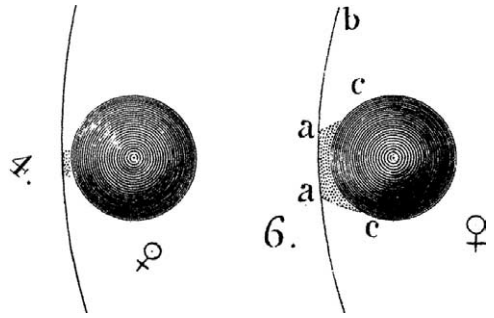


Fig. 1. Bergman (1761–1762) rendition of the Black Drop effect during the 1761 transit of Venus. Reprinted with permission from the Royal Society.

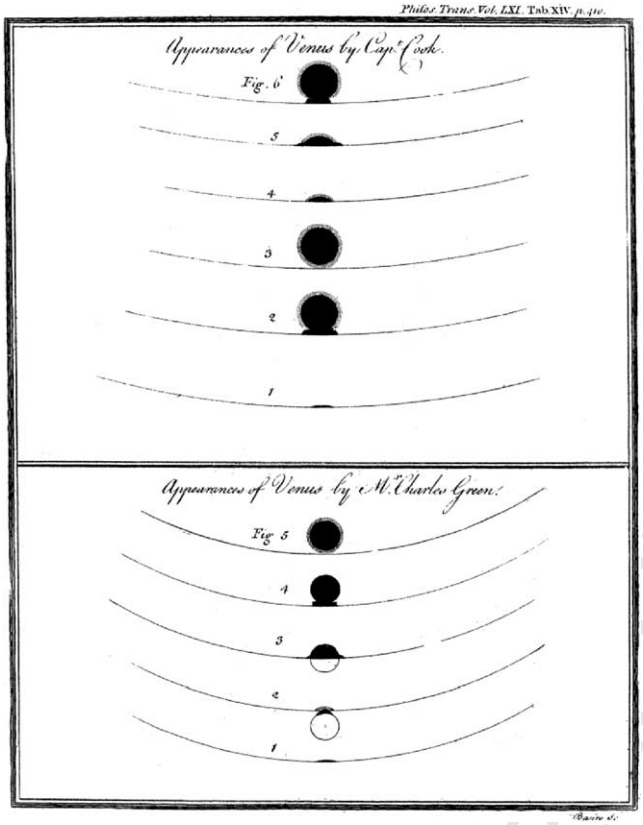


Fig. 2. The Black Drop effect as depicted by Cook and Green (1771) from their observations of the 1769 transit of Venus. Reprinted with permission from the Royal Society.

perished from malaria and dysentery in the service of science. The travails of Le Gentil on his unsuccessful 12-year expedition to Asia, for the 1761 and 1769 events, were especially poignant (Fernie, 1997–1999; Fernie, 2002). Halley and others worked out methods for determining the absolute scale of the Solar System by accurately timing the duration of the approximately 6-hour passage of Venus across a chord on the solar disc. Photographic methods were in use by the transits of 8–9 December 1874 and 6 December 1882 (Fig. 3). The many expeditions to observe these 18th and 19th century events were described by Woolf (1959), Chapman (1998), Dick et al. (1998), Maunder and Moore (1999), Maor (2000), Sellers (2001). The 6 December 1882 event was the most recent transit of Venus visible from Earth. The forthcoming events on 8 June 2004 and 5–6 June 2012 will present the first opportunities for observations with modern ground and space based instrumentation (yielding both high angular resolution and rapid temporal cadence).

Transit-based measurement accuracies of the Astronomical Unit were bedeviled by the appearance of the Black Drop effect, wherein a dark ligature emerged apparently joined the disk of a transiting planet to the solar limb. The manifestation of the Black Drop hindered the determination of the precise instants of interior contacts (Woolf, 1959), thus limiting the accuracy of the AU. Schaefer (2001a, 2001b) reviewed the subject and has shown, in the case of Venus, that common explanations of the Black Drop effect, involving light diffraction around the planetary disk or refraction through its atmosphere as well as an "optical illusion," are incorrect. He discussed the explanation in terms of smearing of the image by atmospheric seeing, an idea first advanced by La Lande and Messier (1769) from the 1769 transit. Space-based transit observations are inherently devoid of (time variable) atmospheric seeing effects, as were previously modeled for ground-based observations and discussed by Whittmann (1974).

Mercury, which has no atmosphere of significance, transits the Sun 13 or 14 times a century and did so on 15 November 1999. We have taken advantage of the solar optical imaging capabilities of the Transition Region and Coronal Explorer (TRACE) spacecraft, unfettered by the Earth's atmosphere, to obtain high-resolution imagery of the limb-transit ingress. We have used these space-based observations of the transit of Mercury to unequivocally demonstrate the definitive cause of the Black Drop effect and elaborate on the (relatively insignificant) effects of diffraction (as is also applicable in the case of Venus).

## 2. Observations and data reduction

We obtained TRACE "White Light" (WL[1] = 1200–9600 Å) images of the ingress phase of the 15 November 1999 transit of Mercury (Fig. 5). Mercury's angular diameter at the time of ingress was 9.86″ (4880 km at 0.6768 AU, imaged across 20 detector pixels) as seen from TRACE's position in its low-Earth orbit. The WL PSF is highly stable,[2] but the effective TRACE optical resolution is Nyquist-limited by the 0.5″ pixels$^{-1}$ sampling of its CCD (Handy et al., 1999) rather than diffraction-limited ($\lambda_{6200\,\text{Å}}/2D = 0.5''$) by its 30 cm telescope. Hence, the diameter of the disk of Mercury was resolved by ∼ 10 band-integrated WL resolution elements.

[1] The TRACE WL instrumental sensitivity extends from ∼ 0.12–1.0 μm, as shown in Fig. 4 in response to an un-limb darkened solar spectrum.

[2] http://vestige.lmsal.com/TRACE/Project/Instrument/inssumma.htm.

S0019-1035(03)00384-1/FLA AID:7261 Vol.●●●(●●●)
ELSGMLTM(YICAR):m5 2003/12/18 Prn:8/01/2004; 16:03
yicar7261
P.3 (1-8)
by:Neringa p. 3



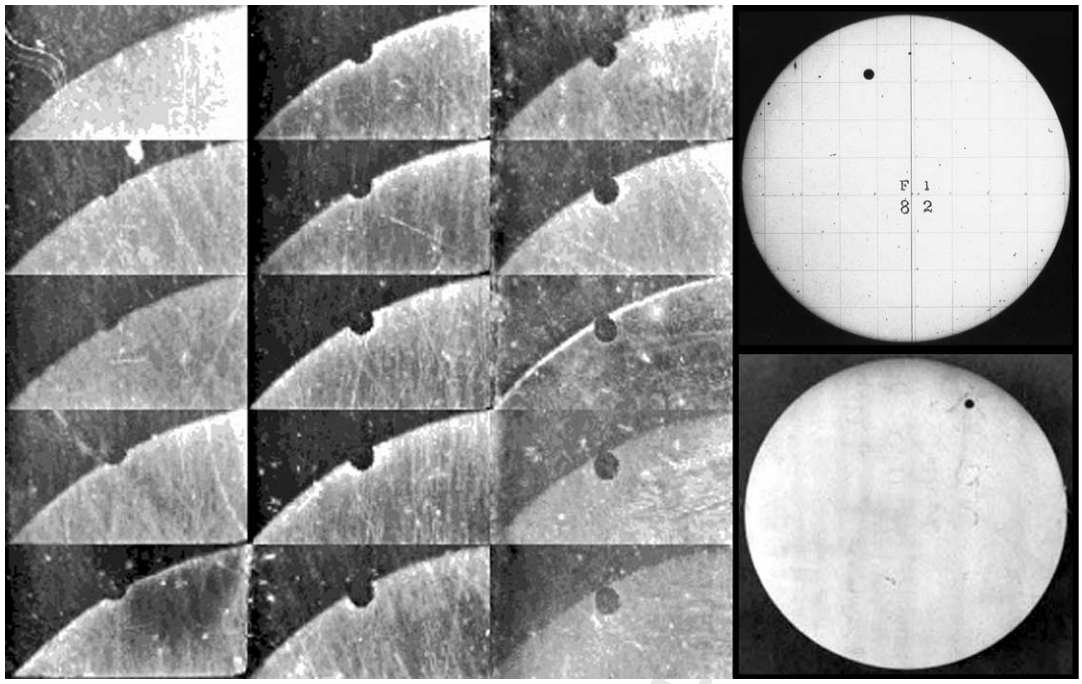


Fig. 3. Photographic images of the 19th century transits of Venus. (Left) Daguerreotypic time-resolved ingress sequence of the 1874 transit by Janssen (1875) using his "photographic revolver" (http://web.inter.nl.net/users/anima/chronoph/index.htm) (Janssen, 1873, 1876; Anonymous, 1875; Canales, 2002). (Right) The 1882 transit; one of eleven surviving images taken by the United States Naval Observatory (top, courtesy of USNO); photograph by Maria Mitchell and her students at Vassar College (bottom, reprinted with permission from Archives and Special Collections, Vassar College Libraries). South is up in both 1882 transit images.

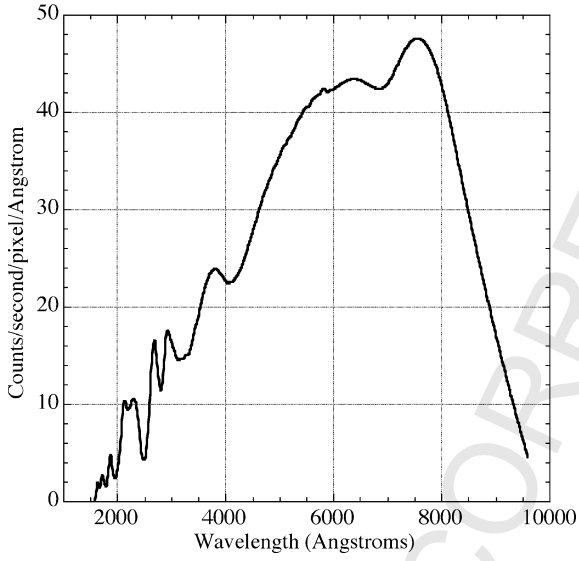


Fig. 4. TRACE "White Light" instrumental response to an un-limb darkened solar spectrum.

Fifty contiguous 384 × 1024 CCD frames (each 3.2 ms exposures separated in time by ∼ 38 s) were selected, completely spanning the photospheric ingress phase of the transit. The raw images were processed with *trace_prep* and *trace_dark-sub* (version 2.00). We followed the method described by Aschwanden et al. (2000) in reducing TRACE data to produce images with dark current removed and pedestal-corrected count rates.

### 2.1. *Post-processing*

Frame-dependent pattern noise (diagonal banding), imprinted on a temporally stable instrumental horizontal signal gradient (and DC bias), remained in the images after applying these basic calibration steps (Fig. 6A). These artifacts were removed from each frame in two steps utilizing, in part, the IDP3[3] (Schneider and Stobie, 2002) and PSPECT[4] (Schneider, 2000) image analysis software. Pattern noise was eliminated by building, and then subtracting, a two-dimensional model image of the banding characterized in frequency, amplitude and phase from an apodized Fourier-transformed power spectrum of the off-disk background region. With the frame-dependent pattern noise removed, all frames were median-combined (Fig. 6B) to obtain a high S/N image of the solar disk and the background "above" the Sun. Time-variable photospheric features (i.e., granulation) are smoothed over the 1871 seconds spanned in the composite frame. A second, two-component higher frequency, frame-independent pattern noise (of too low an amplitude to characterize sufficiently by Fourier analysis in individual frames) is seen in the median combination (Fig. 6B, inset). This high frequency pattern-noise was modeled from off-disk power spectrum of the median combined image, then

[3] ftp://nicmos.as.arizona.edu/pub/NICMOS/software/analysis/idp3.tar.gz.

[4] ftp://nicmos.as.arizona.edu/pub/NICMOS/software/testing/pspect.tar.gz.

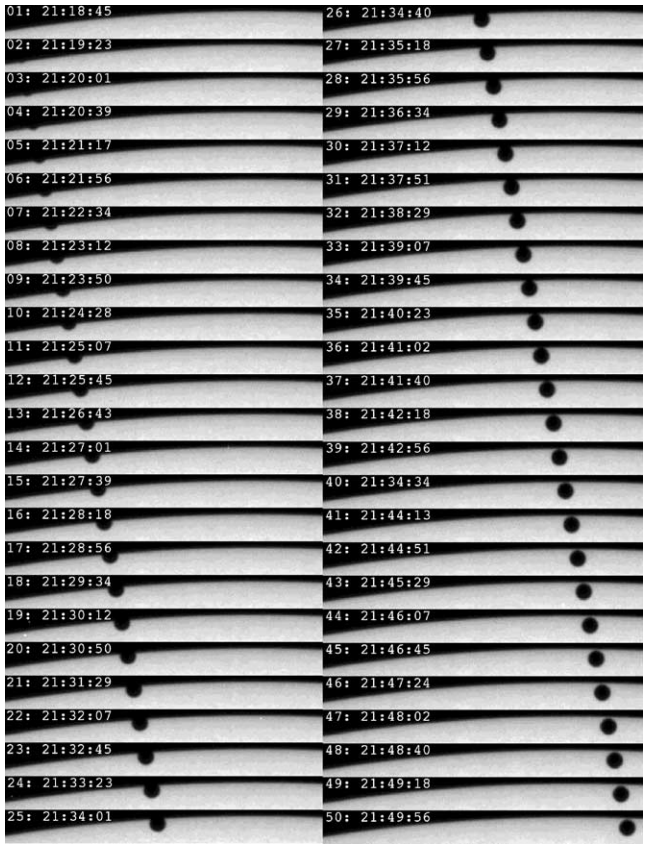


Fig. 5. A series of images of the 15 November 1999 near-grazing transit of Mercury, observed with a temporal cadence of ∼ 38 s, in the TRACE "White Light" band. The images, spanning 21 minutes, fully tile the ingress phase of the transit from 21:18:45 through 21:49:56 UT. Note the emergence and evolution of the Black Drop effect especially beginning at frame 35 (21:40:23 UT) and persisting until the end of the series.

removed from the individual frames in a manner similar to the higher amplitude, lower frequency noise. The horizontal signal gradient was measured from column-medians in the off-disk background after both pattern noise components were removed, and then was column-wise subtracted from the individual frames (Fig. 6C).

With the removal of these artifacts, the image quality was sufficiently improved to examine the nature of the Black Drop effect with a differential photometric accuracy of a few percent (Figs. 6D and 6E). The Black Drop effect, while less significant than in most ground-based images, where the typical time-variable daytime "seeing" disk is a few times larger than the TRACE resolution, is readily apparent in the spacecraft images. The isophotal contours in Fig. 6E clearly show the morphology of the phenomenon.

### 2.2. Solar limb darkening

Because the edge of the solar disk is limb darkened, the (back-lit) illumination function for the mercurian disk is radially asymmetric (Fig. 7). The anisotropic surface brightness of the illumination function (that is, of the photosphere) must be considered in convolution with the TRACE instrumental point-spread function (PSF) to understand (and to reproduce, or remove) its contribution to the Black Drop effect. The TRACE WL PSF has a very nearly Gaussian core and, in analytic form, its higher order Airy structure is well represented by the classical diffractive prescription of a centrally obscured circular aperture. In all that follows, we adopt this simple, but high fidelity surrogated to a more detailed (but unavailable) mapping of the TRACE WL PSF.

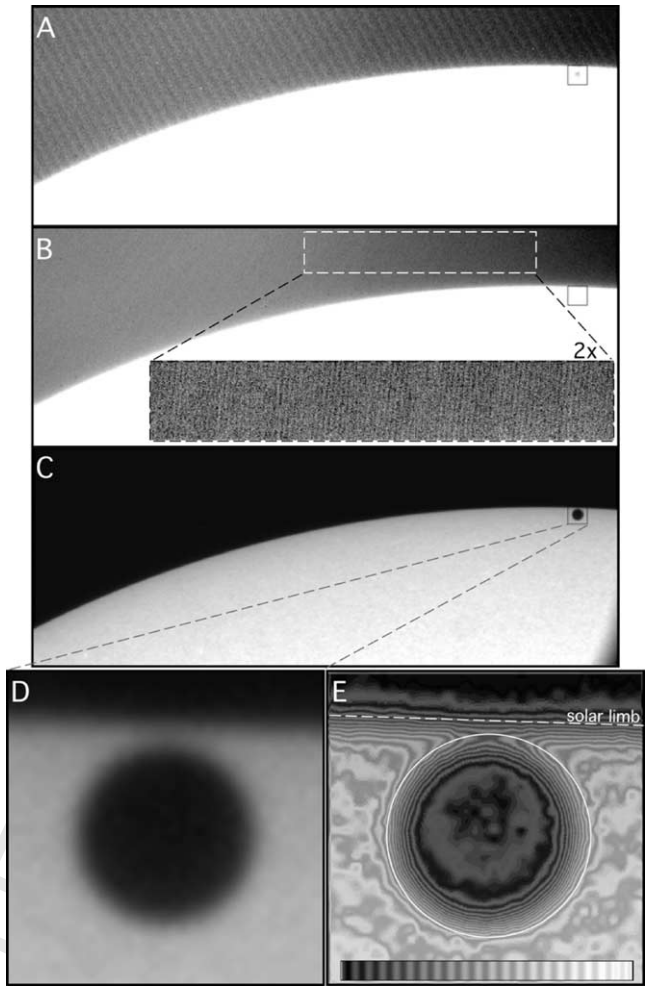


Fig. 6. Post-processing of a representative image (frame 50, 21:49:56 UT) to remove image artifacts. (A) Before post-processing, frame-dependent pattern noise and horizontal signal gradient degrading the image is readily apparent. (B) Median combination of all 50 frames, after removing frame-dependent pattern noise (inset at 2× and horizontal intensity gradient removed and intensity re-scaled to illustrate higher frequency noise). (C) Final post-processed individual frame (compare to (A)) after removing frame-independent high frequency noise and horizontal signal gradient. (D) Enlargement of the disk of Mercury in silhouette. The Black Drop effect is darkened region between the "upper" part of the mercurian disk and the solar limb, also shown isophotally in panel (E).

To remove the heliocentrically radial effects of limb darkening (Fig. 8), we built and subtracted a model image of the PSF-broadened azimuthally averaged photospheric brightness profile from each image. This process collapses the radial dynamic range so that the mean intensities in any regions of the photosphere (averaged over spatial scales larger

S0019-1035(03)00384-1/FLA AID:7261 Vol.●●●(●●●)
ELSGMLTM(YICAR):m5 2003/12/18 Prn:8/01/2004; 16:03
yicar7261
P.5 (1-8)
by:Neringa p. 5



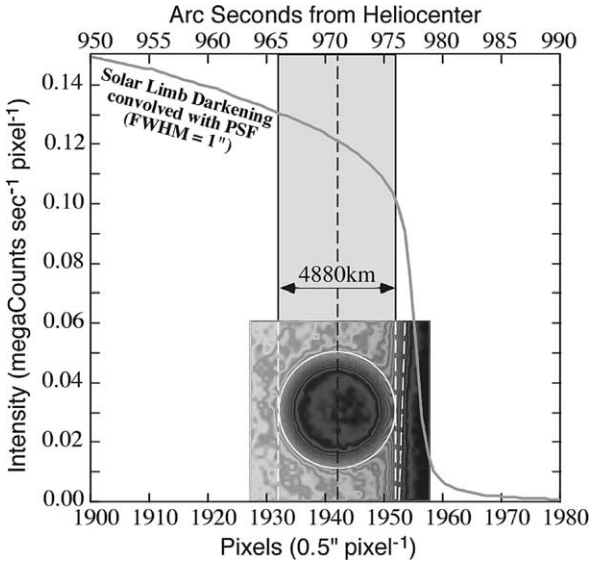


Fig. 7. Solar limb darkening as it affects the Black Drop effect. The observed limb-darkening profile (implicitly convolved with the TRACE white-light point-spread function) is measured from a heliocentric azimuthally medianed radial intensity profile from the median combined image shown Fig. 6B and is over-plotted to scale with the mercurian disk.

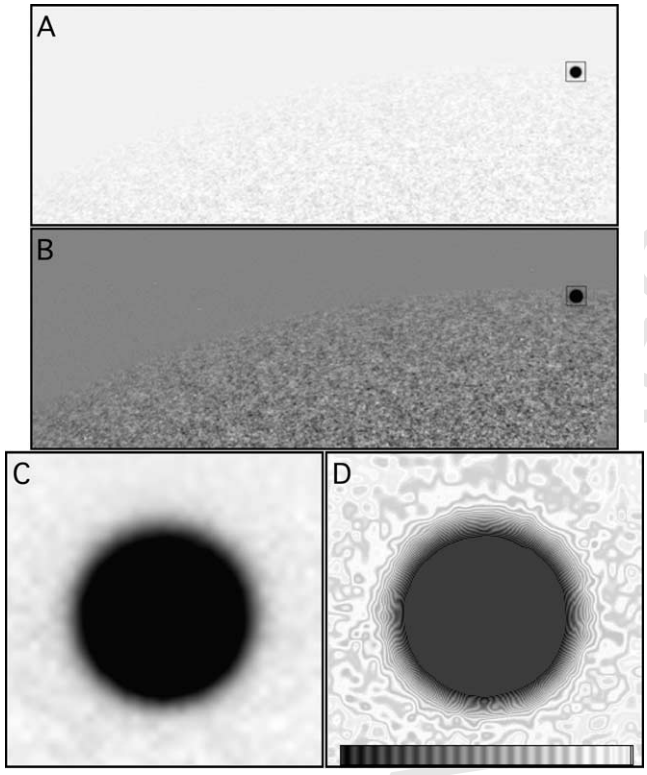


Fig. 8. The result of subtracting the PSF-broadened azimuthally averaged photospheric brightness profile from each image (A). The image below (B) is stretched to better show the mercurian disk and photospheric granulation. The images of the mercurian disk are enlarged in (C) and (D).

than the photospheric structures, and except where Mercury appears) and of the background are equal. By doing so, we eliminated the underlying PSF-broadened heliocentric radial

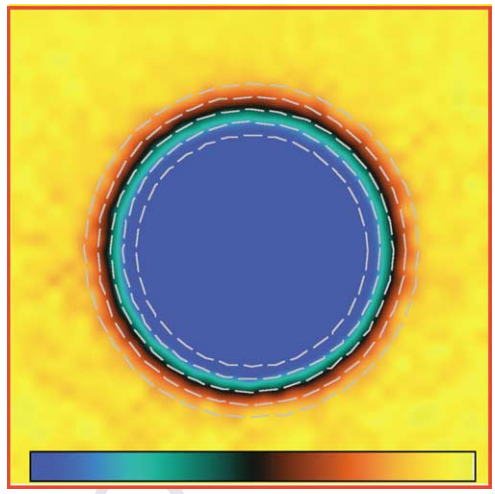

Fig. 9. The 0.8–1.2$r_{\mathrm{mercury}}$ ellipse fit solutions (at 0.1$r_{\mathrm{mercury}}$ intervals) overlaid on the processed image from 21:49:56 UT.

brightness gradient and the brightness discontinuity at the solar limb boundary.

The globally background-flattened silhouetted images of the mercurian disk (e.g., Fig. 8C) show no evidence of the Black Drop effect. While the edge of the mercurian disk is blurred by the instrumental PSF, intrinsic background brightness variations from photospheric granulation (e.g., Fig. 8D) dominate the uncertainties in re-measuring the circum-mercurian intensity isophotes. Compare, respectively, Figs. 6C and 6D (observed, before subtraction) to Figs. 8C and 8D (after correcting for PSF-broadened limb darkening). Instrumental "blurring" by the TRACE PSF is repeatable due to the stability of the platform, unlike otherwise analogous atmospheric blurring in (seeing-limited) ground-based observations.

With the limb-darkened solar photosphere and the off-disk background flattened as described, the intensity isophotes around the mercurian disk were statistically indistinguishable from circularly symmetric as determined from least-squares ellipse-fitting (Fig. 9).

### 2.3. *Image deconvolution*

After removing the effects of the PSF-broadened limb-darkened background, the observed mercurian disk (Fig. 10A) is itself still broadened in convolution with the TRACE WL PSF. To quantify the magnitude of this effect we deconvolved our post-processed images (Figs. 10B–10E) via a modified form of the Richardson–Lucy (RL) method[5] (Snyder, 1990). For the deconvolution kernel we built polychromatic model PSFs (Fig. 10D) as the linear superposition monochromatic PSFs, spaced by 50 Å (∼ 1% of the central wavelength of the band pass), and intensity-weighted by the product of the instrumental response function and the

[5] ftp://nicmos.as.arizona.edu/pub/NICMOS/software/analysis/lucy.tar.gz.

S0019-1035(03)00384-1/FLA AID:7261 Vol.●●●(●●●)
ELSGMLTM(YICAR):m5 2003/12/18 Prn:8/01/2004; 16:03
yicar7261
P.6(1-8)
by:Neringa p. 6



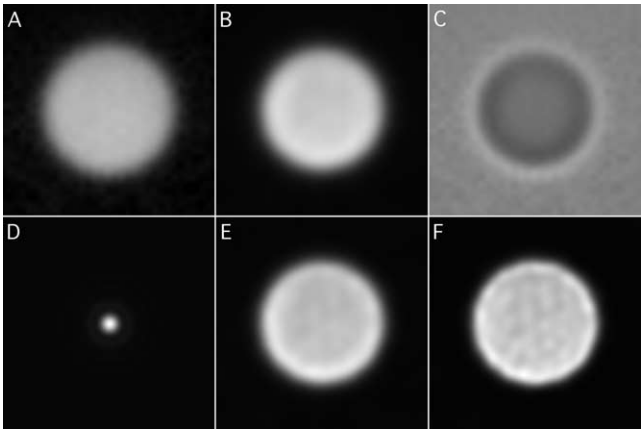


Fig. 10. Image deconvolution by the RL method. (A) Observed image of mercurian disk in silhouette (inverted) after removing the limb-darkened background. (B) After 10 RL iterations. (C) Residuals (A)–(B). (D) The Gaussian core of the model PSF (indicative of the size of a resolution element). (E) and (F) After 20 and 50 RL iterations, respectively.

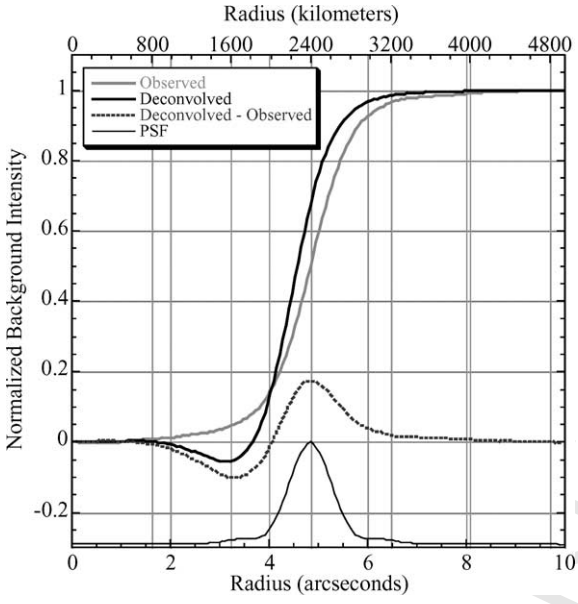


Fig. 11. Azimuthally medianed radial profiles of the observed and deconvolved images of the mercurian disk (corresponding to Figs. 8A and 8C), the TRACE WL model PSF and the residuals.

radially dependent spectral energy distribution of the limb darkened solar photosphere. PSF broadening, which blurs the limb, also darkens the region interior to it, and brightens the exterior region (Fig. 10C).

We compared the azimuthally medianed radial profile of Mercury before and after ten damped iterations of the RL deconvolution procedure (Fig. 11) and found the planet's photometric radius $\sim 0.55''$ ($\sim 270$ km) narrower in the deconvolved image. This result was repeatable for all of the WL images during, and after, the photospheric limb transit of Mercury. Because the TRACE PSF is both temporally stable and critically sampled by the detector, image deconvolution (in high S/N images such as these) is a pathway to improving on the instrumentally limited spatial resolution. These results may be improved further by the application of a higher fidelity representation of the TRACE WL PSF in the deconvolution process.

### 2.4. Residual edge "softening" and diffraction

The edge of the mercurian disk is not geometrically sharp even after fifty iterations of the damped RL deconvolution procedure (Fig. 9F), but has a residual photometric half-width of $\sim 1.13$ pixels ($0.56''$), $\sim 6\%$ of Mercury's diameter. Some of this may be attributed to instrumental scattering and some due to the imperfect fidelity of the model PSF employed in the deconvolutions, though other contributory mechanisms may exist. For example, sunlight is diffracted around the edge of the mercurian disk and reaches the observer along lines-of-sight which would otherwise be in the geometrical shadow of Mercury. Hence, the disk does not appear to be uniformly dark, in part, because the mercurian disk seen in silhouette acts as a diffracting aperture. It was previously suggested that diffraction of sunlight by the back-lit mercurian disk is inconsequential in considering the Black Drop effect (Schaefer, 2001a, 2001b). To evaluate this conjecture, we performed a numerically rigorous two-dimensional polychromatic diffraction calculation. We examined the effect of Fresnel diffraction under the broad pass band of the TRACE WL instrumental response (independent of the instrumental PSF), and found that while still of very little consequence, the effects of edge diffraction were underestimated by Schaefer. In our diffractive calculations we treated the illumination function as a dense rectangular grid of polychromatic point sources tiling the mercurian disk (10 mas inter-point spacing; 5 km at the distance of Mercury). We computed the wavelength-dependent intensity of all points in a grid of circum-mercurian field points as a function of their positions with respect to the geometrical edge of the planet's disk and their distance from the solar limb (Evans, 1970; Nather and McCants, 1970). In doing so, before co-addition, we intensity-weighted every point in each of the 168 (50 angstrom wide) wavelength intervals by the product of the TRACE instrumental response (sensitivity) function and a limb-darkened solar spectrum (for several positions of Mercury near the solar limb).

We characterize the "sharpness" of the rising radial edge of the resulting two-dimensional intensity pattern as the distance between the point of geometrical tangency of the line-of-sight to the mercurian limb and the point at which the intensity has risen (before the first spatially and polychromatically broadened diffractive maximum) to its unocculted intensity (Schneider, 1985). This distance is $\sim 43$ km at the distance of Mercury (though, in detail, this is somewhat dependent upon Mercury's position on the limb-darkened disk). This is only $\sim 1/6$ of a TRACE pixel, or $\sim 9\%$ the width a WL resolution element, and hence is observationally undetectable, and not a significant contributor to the Black Drop effect.

S0019-1035(03)00384-1/FLA AID:7261 Vol.●●●(●●●)
ELSGMLTM(YICAR):m5 2003/12/18 Prn:8/01/2004; 16:03
yicar7261
P.7 (1-8)
by:Neringa p. 7



## 3. Conclusion

The principal cause of the Black Drop effect, which has historically impeded ground-based planetary transit measurements, is optical broadening resulting from the convolution of the systemic PSF with the planetary and limb-darkened solar disks. TRACE observations are free from PSF instabilities caused by "seeing" in the terrestrial atmosphere and allow mitigation of the Black Drop effect from the intrinsic disk images. Such stable, critically sampled, near diffraction-limited images may be further enhanced by PSF deconvolution, enabling very high-precision differential astrometric position measures.

Space-based observations of the upcoming transits of Venus may be improved significantly by the methods discussed and by understanding the problem. These methods may enable similar corrections to be made to transit imagery (and spectroscopy) acquired from ground-based facilities augmented with adaptive optics. Adaptive optics improves upon the instantaneous size of the natural daytime seeing disk, though temporal stability of the PSF remains an issue resolved only by space-based observations.[6] The need for such imaging observations to calibrate the Keplerian distance scale has been obviated by other methods, though such observations will likely be carried out for historical liaison. The beginning and end of the 2004 transit will be visible from Europe and Asia, respectively, and intermediate locations will be able to duplicate the methods of historical expeditions by observing the transit over its entire 6-hour period.[7,8,9] Beyond the historical interest and underpinning, the ability to decouple and compensate for PSF-broadened solar limb darkening from the UV/optical absorption (and refractive effects) through the cytherean atmosphere will greatly enhance the ability to use such observations to probe azimuthally anisotropic properties of the planet's atmosphere along the line-of-sight. The 8 June 2004 transit will present the first opportunity ever for such space-based observations.

## Acknowledgments

This work was supported in part by NSF grant ATM-000545; Pasachoff's work on eclipses has also been supported in part by the Committee for Research and Exploration of the National Geographic Society. He is grateful for sabbatical hospitality to Harvey Tananbaum and Ramesh Narayan at the Harvard–Smithsonian Center for Astrophysics. TRACE is supported by a NASA/GSFC contract to the Lockheed Martin Corp. Extensive use of analysis software developed by the NICMOS IDT under NASA grant NAG 5-3042 is acknowledged. We are indebted to Ted Tarbell for his helpful commentary on several issues discussed in this paper and for supplying clarifying information in regard to the TRACE WL sensitivity function.

[6] http://www.stsci.edu/spd/cycle12/NICMOS_AO_WHITEPAPER.html.
[7] http://www.williams.edu/astronomy/eclipse/transitVenus.htm.
[8] http://www.eso.org/outreach/eduoff/vt-2004/.
[9] http://www.transitofvenus.org.

## References

Albers, S., 1979. Mutual occultations of planets: 1557 to 2230. Sky Telescope 57, 220–222.

Anonymous, 1875. Sectional proceedings, section A—mathematics and physics. Nature 12, 405.

Aschwanden, M.J., Nightingale, R.W., Tarbell, T.D, Wolfson, C.J., 2000. Time variability of the "Quiet" Sun observed with TRACE. I. Instrumental effects, event detection, and discrimination of extreme-ultraviolet microflares. Astrophys. J. 535, 1027–1046.

Bergman, T., 1761–1762. An account of the observations made on the same transit at Upsal in Sweden: in a letter to Mr. Benjamin Wilson, F.R.S. from Mr. Thobern Bergman, of Upsal. Philos. Trans. 52, 227–230.

Bevis, J., 1737–1738. Mercurius a Venere occultatus Maii 17 1737 in Observatorio Regio Grenovici, ab J. Bevis, M.D. Observatus. Philol. Trans. 40, 227–230, 394–395.

Bevis, J., 1742–1743. Epistola Johannis Bevis, M.D. ad Gul. Jones, Armig. R.S.S. de transitibus Mercurii sub Sole, Oct. 31 1736 et Oct. 25 1743. Philos. Trans. 42, 622–626.

Canales, J., 2002. Photographic Venus: the 'Cinematographic Turn' and its alternatives in nineteenth-century France. Isis 93, 585–613.

Chapman, A., 1998. The transits of Venus. Endeavour 22, 148–151.

Cook, J., Green, C., 1771. Observations made, by appointment of the Royal Society, at King George's Island in the South Sea; by Mr. Charles Green, formerly assistant at the Royal Observatory at Greenwich, and Lieut. James Cook, of His Majesty's Ship the Endeavour. Philos. Trans. 61, 397–421.

Dick, S.J., Orchiston, W., Love, T., 1998. Simon Newcomb, William Harkness and the nineteenth-century American transit of Venus expeditions. J. Hist. Astron. 29, 221–255.

Evans, D.S., 1970. Photoelectric measurement of lunar occultations III. Lunar limb effects. Astron. J. 75, 589–599.

Fernie, J.D., 1997–1999. Transits, travels and tribulations. Am. Sci. I. 85 (1997) 120–122. II. 85 (1997) 418–421. III. 86 (1998) 123–126. IV. 86 (1998) 422–425. V. 87 (1999) 119–121.

Fernie, J.D., 2002. Setting Sail for the Universe: Astronomers and Their Discoveries. Rutgers Univ. Press, Piscataway, NJ.

Ferguson, K., 1999. Measuring the Universe. Walker & Co., New York.

Handy, B.N., et al., 1999. The transition region and coronal explorer. Solar Phys. 187, 229–260.

Hughes, D.W., 2001. Six stages in the history of the astronomical unit. J. Hist. Astron. 4, 15–28.

Janssen, P.C.J., 1873. Passage de Vénus: method pour obtenir photographiquement l'instant des contacts avec les circonstances physiques gu'il présentent. C. R. Acad. Sci. 76, 677.

Janssen, P.C.J., 1875. Le passage de Vénus, résultat des expédition Française. Nature 8.

Janssen, P.C.J., 1876. Présentation du revolver photographique et épreuves obtenues avec cet instrument. Bull. Soc. Fr. Photogr. 22.

Kilburn, K., Pasachoff, J.M., Gingerich, O., 2003. The forgotten star atlas: John Bevis's Uranographia Britannica. J. Hist. Astron. 29, 125–144.

La Lande, J.-J., Messier, C., 1769. Observations of the transit of Venus on June 3, 1769, and the eclipse of the Sun on the following day, made at Paris, and other places. Philos. Trans. 59, 374–377.

Maunder, M., Moore, P., 1999. Transit: When Planets Cross the Sun. Springer-Verlag, Berlin.

Maor, E., 2000. June 8, 2004—Venus in Transit. Princeton Univ. Press, Princeton, NJ.

de Meis, S., 1993. Some mutual planetary occultations. BJAA 103, 185.

Nather, R.E., McCants, M.M., 1970. Photoelectric measurements of lunar occultations. IV. Data analysis. Astron. J. 75, 963–968.

Pasachoff, J.M., 2000. A Field Guide to the Stars and Planets. Houghton Mifflin, Boston.

Pasachoff, J.M., 2002. Astronomy: From the Earth to the Universe, sixth ed. Brooks/Cole, Pacific Grove, CA.

Schaefer, B.E., 2001a. The transit of Venus and the notorious black drop. Bull. Am. Astron. Soc. 332, 1383. Abstract.

Schaefer, B.E., 2001b. The transit of Venus and the notorious black drop effect. J. Hist. Astron. 32, 325–336.

Schneider, G., 1985. The observation and analysis of lunar occultations of stars with an emphasis on improvements to data acquisition instrumentation and reduction techniques. PhD thesis. University of Florida.

Schneider, G., Pasachoff, J.M., Golub, L., 2001. TRACE observations of the 15 November 1999 transit of Mercury. Bull. Am. Astron. Soc. 33, 1037. http://nicmosis.as.arizona.edu:8000/POSTERS/TOM1999.jpg.

Schneider, G., 2000. Results from the NCC/NICMOS spare detector June 2000 EMI Test, STScI Instrument Science Reports, NICMOS ISR 2000-006. http://www.stsci.edu/hst/nicmos/documents/isrs/isr2000_006.pdf.

Schneider, G., Stobie, E., 2002. Pushing the envelope: unleashing the potential of high contrast imaging with HST. ASP Conf. Ser. 281, 382–386.

Sellers, D., 2001. The Transit of Venus—The Quest to Find the True Distance of the Sun. MagaVelda Press, Leeds.

Snyder, D.L., 1990. Modifications of the Lucy–Richardson iteration for restoring Hubble Space Telescope imagery. In: Proc. STScI Workshop on the Restoration of HST Images and Spectra, pp. 56–61.

Van Helden, A., 1989–1995. Measuring solar parallax: the Venus transits of 1761 and 1769 and their nineteenth-century sequels. In: Taton, R., Wilson, C., (Eds.) The General History of Astronomy, II: Planetary Astronomy from the Renaissance to the Rise of Astrophysics. Cambridge Univ. Press, Cambridge, p. 156.

Whittmann, A., 1974. Numerical simulations of the Mercury transit black drop phenomenon. Astron. Astrophys. 1, 239–243.

Woolf, H., 1959. The Transits of Venus: A Study in Eighteenth Century Science. Princeton Univ. Press, Princeton.